

CHAPTER 4

DETERMINATION OF SHAPE AND SIZE OF CANOPY OF MAIN PARACHUTE

Notations

β	Power of parachute filling function
ρ	Density (kg/m ³)
m	Total recovery mass (kg)
n	Parachute filling parameter
t	Time (s)
q	Dynamic pressure ((N/m ²)
h	Altitude (m)
x	Horizontal axis in local coordinate system
F_D	Drag force (N)
S	Parachute surface area (m ²)
T	Temperature (°C)
V	Velocity m/s)
C_D	Drag coefficient
D_o	Parachute nominal diameter (m)
t_f	Canopy filling time (s)
V_0	Velocity at the end of line stretch

4.1 Introduction

Main parachutes are used as a final decelerator for landing of space payload, providing stability and desired descend rate. Selection of main parachute is most critical and has final hope for success of mission, its size is restricted by landing speed, and weight is restricted by available textile materials and must have high reliability. Therefore, in this chapter, an investigation has been carried out on shape of main parachute and detailed selection criteria considering recovery of re-entry space payload considering the 500 kg (unmanned) and 3500 kg (manned) class. Based on size of the parachute, canopy filling time, velocity reduction, peak deceleration, opening shock, a unique type of solid canopy with slots rather than a complex Ringsail canopy as used by other missions is proposed. This new concept of parachute has been designed, developed, and used in maiden flight of space capsule in low earth orbit to qualify complete system for proposed Indian human space program.

Parachutes are used in various manned and unmanned space payload recovery experiments because of lighter weight, high strength to weight ratio and high-performance reliability. Space programmes like Space Recovery Experiment (SRE, India), Apollo (USA), SOYUZ (Russia), Shenzhou (China) are some of the few examples where parachutes have been successfully used for landing on earth after completion of space mission. In any human space programs, recovery capsule invariably contains two to three stages of parachutes consisting pilot, drogue and main parachutes. Main Parachutes are used to decelerate the crew module for landing to a terminal speed that ensures astronaut safety.

In literature, it is found that Apollo Parachute Landing System (Knacke, 1968) was the most advanced, thoroughly engineered and rigorous tested system. The parachute system stabilizes and decelerates the crew carrying Apollo command module (5.9-ton payload)

after the mission is completed to a descend velocity suitable for water landing. In this program, cluster of three main parachutes, Ringsail canopy having size 26.25 m was used. The selection of parachute for Apollo was done after successful performance perceived in Mercury and Gemini landing systems. The Gemini (John, 1966) landing system uses 25.85 m canopy diameter Ringsail parachute for terminal descent. The Chinese Shenzhou (GUO et al., 2011) manned spacecraft resembled the Russian Soyuz spacecraft (wikipedia.org/wiki/Soyuz) but Shenzhou parachute was larger in size and all-new construction. The Shenzhou capsule employed the same landing technique as Soyuz. Single drogue, followed by a single main parachute, Ringsail type, area of 1200 m² used. J. Rives (2011) has shown experimental results for the recovery of 2800 kg Apollo type re-entry payload. The cluster of three tri-conical parachutes (22.9 m) has been used as a main decelerator. In many planetary exploration missions, conical ribbon and Disc-Gap-Band (DGB) parachutes were frequently used due to low opening shock, quick opening and stability in terms of oscillation, few are listed in the Table 4.1 and their shape of canopy shown in Figure 4.1. It clears from the Table 4.1 and Figure 4.1 that flat circular solid canopy had not been used so far for manned space mission.

Table 4.1: Worldwide parachutes used in planetary exploration missions

Mission	Destination	Main parachute
VIKING	MARS	16.2 m, DGB
PIONEER VENUS	VENUS	4.94 m, Conical ribbon
GALILEO	JUPITER	3.8 m, Conical ribbon
MARS PATHFINDER	MARS	12.7 m, DGB
MER	MARS	8.3 m, DGB
CASSINI/ HUYGENS	SATURN/ TITAN	14.1 m, DGB



Figure 4.1: Commonly used canopies in planetary exploration missions

Mohaghegh (2007) has shown that the filling time is a major criterion to classify the parachute types. In manned space mission, the module recovery is required to be proven for both normal and launch Pad abort situations and quick filling of canopy providing minimum loss of altitude during inflation of the parachute. The peak deceleration due to rapid parachute inflation is also one of the major criteria for the selection of parachute for manned spaceflight programs. The maximum g-level during deceleration should be as low as possible and can be tolerated by human. At higher dynamic pressure, slotted type parachutes are used whereas at lower dynamic pressure, shape optimization and more option is available to select the parachute type. Maximum velocity for main parachute deployment in manned space mission world wide is 80 m/s and 3 km altitude. In this chapter, same deployment conditions of main parachute is considered for the analysis and used in pre-flight qualification testings.

Indian first space mission, SRE (Sidana *et al.*, 2005) unmanned re-entry payload (500 kg) was successfully launched and recovered in January 2007. It consists of two stage parachutes, one pilot and one main parachute (aero-conical parachute, size 12.44 m) and forced inflation floatation system for afloat the capsule on sea. To meet the parachute

reliability, rigorous testing on parachute was done from model analysis to dynamic tests and subsequently helicopter drop test before using in the final flight. The SRE mission was successful without using any standby decelerator system unlike Apollo and Soyuz. After success of SRE, next mission for human space program is planned. This chapter, main focus is given to selection of main parachute for 3500 kg space payload. After establish the reliability of parachute, maiden flight was also successfully conducted in low earth orbit.

4.2 Mathematical Modelling

To understand the effect of various parameters on selection of parachute, a point-mass trajectory is simulated. When a parachute deployed in the air, it passes through packed condition to full inflation.

4.2.1 Basic Equilibrium Equations

Calculation of parachute deployment parameters requires the numerical solution to the equations of motion for a viscous, turbulent, separated airflow at instant of time and altitude changes. It can be described by a mathematical model, simplification must be made, as long as the model can be validated satisfactorily by experiment or by comparison with reference data. Following assumptions are made for framing the mathematical equations.

Assumptions

Following assumptions are made to simplify the analysis. However, actual simulation tests will be carried during the dynamic and flight tests.

- (i) 'm' and 'g' are constant

No further mass reduction takes place from 3 km and hence mass and gravity force are assumed to be constant in analysis.

- (ii) Nil wind condition

No side wind effect considered on parachute in the analysis because forward speed of the system at 3 km is very high, however, the system will be tested in actual environment for qualification.

(iii) Flight path angle (γ) is negative

Payload is falling downward so for sake of convenience path angle is assumed negative as shown in Figure 4.2.

(iv) Re-entry payload is stable during main parachute deployment

Stability of the system is controlled by the drogue parachute and bring down the payload in stable condition for opening of main parachute.

Basic equilibrium equations for parachute body mass are written as given in equation (4.1).

$$F_p + F_{CM} = q[(C_{DS})_p + (C_{DS})_{CM}] \quad (4.1)$$

where,

$$q = \frac{1}{2} \rho V^2 \quad \text{and} \quad F_p + F_{CM} = mg$$

4.2.2 Point Mass Trajectory Model

Considering that the parachute payload moving at a flight path angle γ as shown in Figure 4.2. The point mass trajectory equations (4.2 and (4.3) are given as follows.

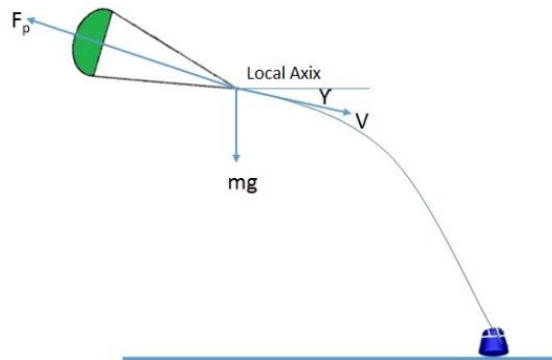


Figure 4.2: Flight path trajectory of re-entry module

Equation of motion, Newton 2nd Law

$$\left. \begin{aligned} \frac{dV}{dt} &= -g \sin \gamma - \frac{F_p}{m} \\ \frac{d\gamma}{dt} &= -\frac{g \cos \gamma}{V} \end{aligned} \right\} \quad (4.2)$$

Kinematics relations

$$\left. \begin{aligned} \frac{dh}{dt} &= V \sin \gamma \\ \frac{dx}{dt} &= V \cos \gamma \end{aligned} \right\} \quad (4.3)$$

The instantaneous drag force generated by the parachute during flight is varying as proportional to the square of the velocity and function of time, as given in equation (4.4).

$$F_p = \frac{1}{2} \rho_{altitude} V^2(t) C_D S(t) \quad (4.4)$$

4.2.3 Drag Area Variation of Parachute

The canopy expansion during inflation is resisted by the structural tension of parachute and inertia until the full inflation occurs. The drag area variation is assumed to be a second order function of time for solid textile canopies and linear function of time for slotted canopies (Macha, 1993). Therefore, for all parachutes, the instant area growth during inflation is given by equation (4.5).

$$C_D S(t) = (C_D S)_0 \left(\frac{t}{t_f} \right)^\beta \quad (4.5)$$

where,

$\beta = 1$, slotted canopy parachute

$\beta = 2$, Solid canopy parachute

The drag area variation with respect to time as written in equation (4.5) has been modeled and analysis carried out in MATLAB. The plot of same is shown in Figure 4.3. This is input for further analysis and selection of main parachute.

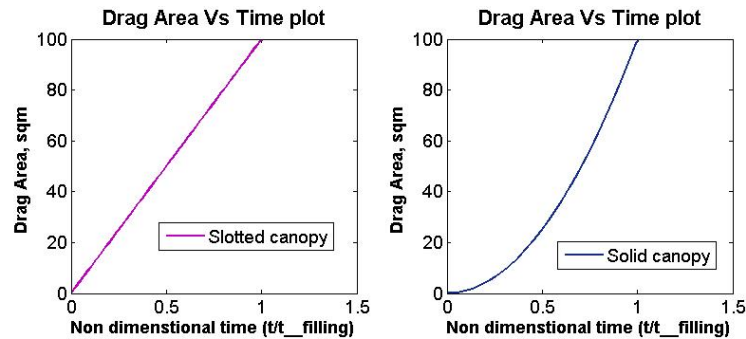


Figure 4.3: Drag area variation for slotted and solid canopy

4.3 Parameters Influencing the Selection of Parachute

The solution of the six types of parachutes for payload mass 500 kg and 3500 kg has been modeled. Analysis for selection of main parachute has been studied based on parachute inflation characteristics, filling time, drag area variation, opening shock and presented in this paper.

4.3.1 Canopy Filling Time

To solve all the above equations, following assumptions and input data have been considered as per specification of mission requirements. Following input data is taken for design analysis:

- (i) Parachute deployment velocity (V_0) = 80 m/s, maximum velocity for main parachute deployment in human space mission used as worldwide. It is due to material availability, reduce the parachute weight and maintain the reliability.

- (ii) Altitude (h) = 3 km (density = 0.9104 kg/m^3), commonly selected altitude for main parachute deployment such as APOLLO, SOYUZ, SHENZHOU space programmes. Above this altitude air density is low and parachute required to be opened at high speed which needs higher strength material and hence it results more weight.
- (iii) $\gamma = -16^\circ$, assumed angle for representation because during main parachute deployment, the re-entry payload may not be falling vertically in all possible scenario.
- (iv) $V_{terminal} = 8 \text{ m/s}$, a safe terminal speed for human tolerance ability and water landing of re-entry payload.

Table 4.2: Drag coefficient and filling time index for various parachutes (Knacke, 1992)

Class	Type	C_D	n_{fill}
Slotted parachutes	Conical ribbon	0.50 to 0.55	14
	Ringsail	0.75 to 0.85	7
	Disc Gap Band	0.52 to 0.58	10
Solid parachutes	Aero-conical	0.635	8
	Tri-conical	0.80 to 0.96	8

Literature has shown that coefficient of drag and filling time index depends on shape of canopy. Table 4.2 shows the slotted and solid canopy used for space applications.

Based on the above inputs and empirical relation (filling time = nD_o/V_o), the canopy filling time of various parachutes estimated for same drag area and deployment condition as shown in Figure 4.4.

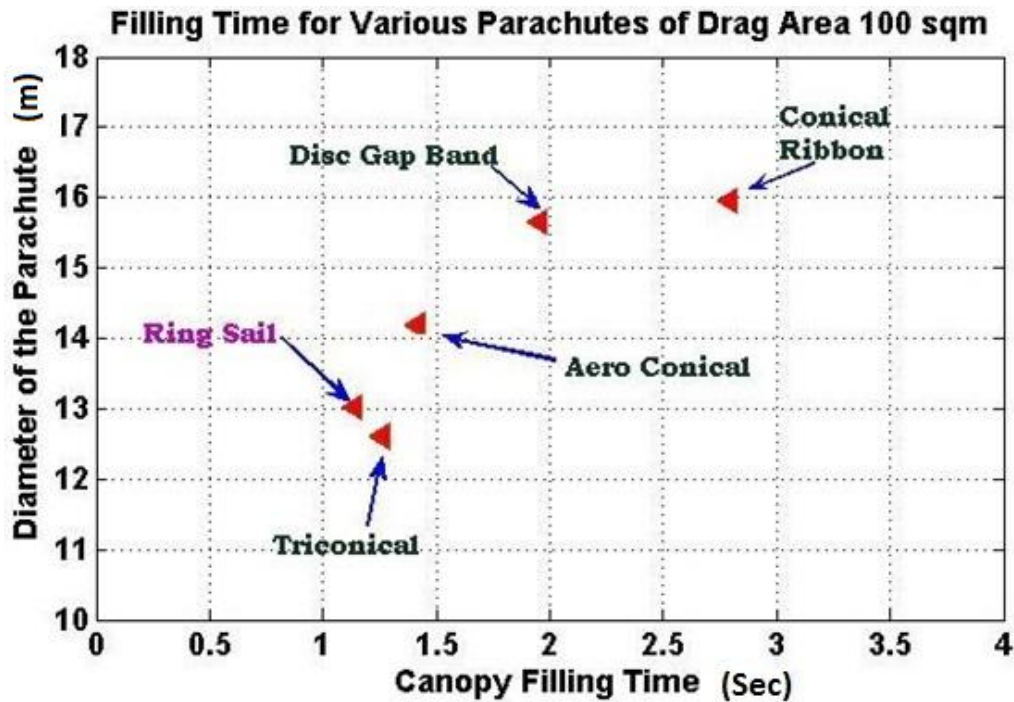


Figure 4.4: Size and filling time of various parachutes ($C_D S = 100 \text{ m}^2$)

Analysis has been carried out for drag area variation and corresponding opening load of Ringsail, aero-conical and conical ribbon and represented in Figure 4.5. It shows that even being a slotted canopy, Ringsail parachute is the fastest opening parachute due to its construction and design. The other solid canopies like tri-conical and aero-conical are having less filling time than the slotted canopies. Drag area growth of conical ribbon is linear and that of for aero-conical parachute is quadratic as shown in Figure 4.5 (a). Due to high filling time index and bigger size of conical ribbon, the filling time is more than that of the aero-conical parachute (Figure 4.4). The C_d of aero-conical parachute is greater than the ribbon parachute. Therefore, the load varies as per size of the parachute as shown in Figure 4.5 (b). That shows that the filling time has direct influence in opening load. This can be seen for Ringsail and aero-conical parachute in Figure 4.5 (b) also.

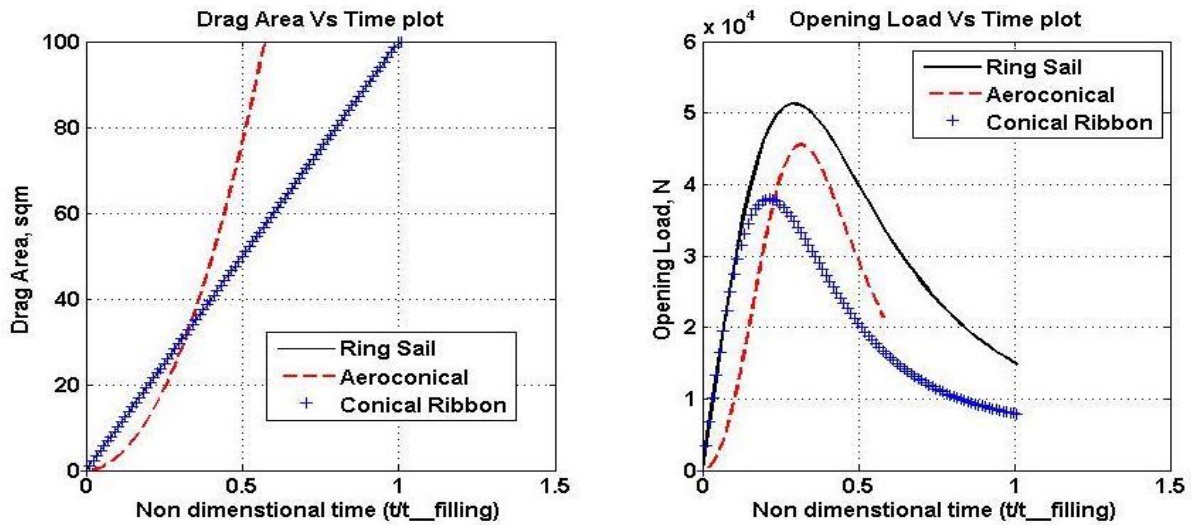


Figure 4.5: (a) Drag area variation vs time plot and (b) Opening load variation vs time plot for ringsail, aero-conical and conical ribbon parachutes (500 kg payload)

The maximum opening load is found in Ringsail parachute due to its fast opening of the canopy and less reduction of velocity as compared to solid canopy as clear from the Figure 4.5 (b).

4.3.2 Parachute Sizing

In this case, C_{Do} , $q_{terminal}$, m and g are known, from equation (4.1) we can find that nominal area of parachute is

$$S_o = (m g / q_{terminal}) / C_{Do}$$

Size estimation for 500 kg and 3500 kg payload class has been carried for various parachutes as shown in Table 4.3. From the Table 4.3, it is clear that ringsail and tri-conical parachute has minimum size and hence less canopy mass which is desirable for any space mission.

Table 4.3: Drag coefficient and size of parachutes

S. No.	Parachute Type	C_D	Estimated Parachute Diameter (m)	
			500 kg payload	3500 kg payload
1.	Conical ribbon	0.50	17.84	47.22
2.	Ringsail	0.75	14.57	38.55
3.	Disc Gap Band	0.52	17.5	46.3
4.	Aero-conical	0.635	15.83	41.89
5.	Tri-conical	0.80	14.11	37.33
6.	Circular slotted solid canopy	0.75	15.88	31

4.3.3 Angle of Oscillation

Angle of oscillation is critical requirement for crew module for safe descent. Figure 4.6 shows wind tunnel data given by Cruz (2008) for angle of oscillation and drag coefficient. Knacke experimental data is also given in Table 4.4. The angle of oscillation in slotted parachute is less than solid canopy parachutes but in cluster, oscillation is absorbed by the canopy interfacing. Therefore, solid canopy is selected for the space mission in configuration of cluster.

Table 4.4: Parachute average angle of oscillation (Knacke, 1992)

S. No.	Parachute Type	Average. Angle of oscillation
1.	Conical ribbon	0 to ± 3
2.	Ringsail	± 5 to ± 10
3.	Disc Gap Band	± 10 to ± 15
4.	Aero-conical(solid)	± 10 to ± 20
5.	Tri-conical (solid)	± 10 to ± 15

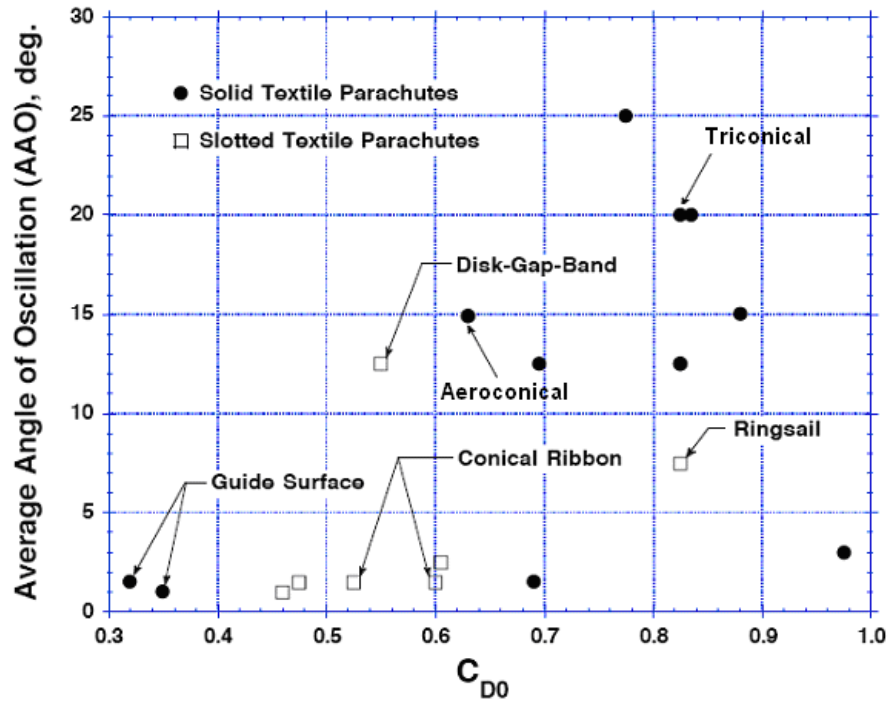


Figure 4.6: Average angle of oscillation vs drag coefficient for slotted and solid canopies

4.3.4 Parachute Opening Shock Load

Selection of material is decided based on maximum opening load that parachute is generating during the deployment. A design analysis for parachute opening load has been done for various types of parachutes considering 500 kg and 3500 kg class payload as shown in Figures 4.7 and 4.8 respectively. The maximum opening load occurs in ringsail parachute whereas in other parachutes, it is lesser and comparable. Effect of payload mass can easily be seen in tri-conical, Disc Gap Band, aero-conical and conical-ribbon. For 500 kg payload, the opening load of tri-conical and aero-conical parachute is higher than the Disc Gap Band and conical ribbon respectively. When the payload mass is increased to 3500 kg, the opening load of tri-conical parachute becomes lower than the Disc-Gap-Band, aero conical and conical-ribbon.

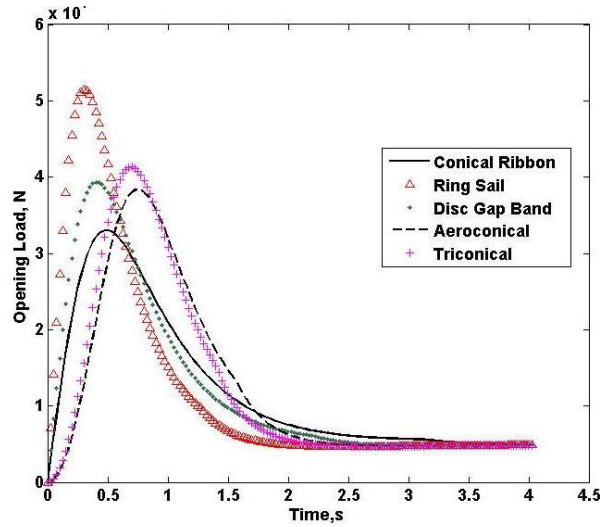


Figure 4.7: Opening load variation of different parachutes for 500 kg payload

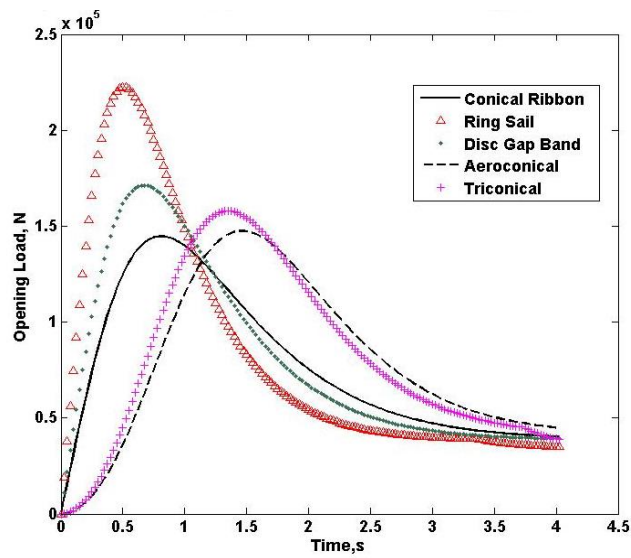


Figure 4.8: Opening load variation of different parachutes for 3500 kg payload

From the equations (4.1), (4.2) and (4.3), analysis of velocity verses time has been carried out in MATLAB and plotted for 500 kg and 3500 kg payloads as shown in Figures 4.9 and 4.10 respectively. The decreasing trend of velocity of payload is due to the inflation characteristics of the individual parachutes. Ringsail parachute reaches nearly terminal

velocity much faster than other parachutes due to lesser inflation time. However, velocity reduction in solid canopy is also comparable.

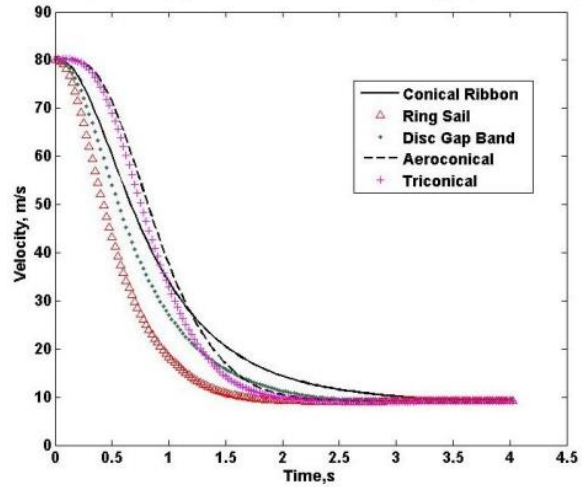


Figure 4. 9: Velocity reduction of different parachutes for 500 kg payload

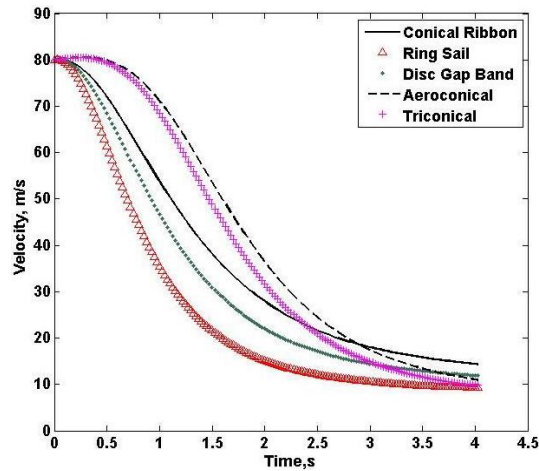


Figure 4.10: Velocity reduction of different parachutes for 3500 kg payload

4.3.5 Peak Deceleration

Deceleration analysis due to main parachute is carried out for 500 kg and 3500 kg payloads as shown in Figures 4.11 and Figure 4.12 respectively. The peak deceleration (in terms of ‘g’ value) for Ringsail parachute is much higher than other parachutes. It is key parameter

for crew carrying module in which the g -level is restricted for the survival of the crew members.

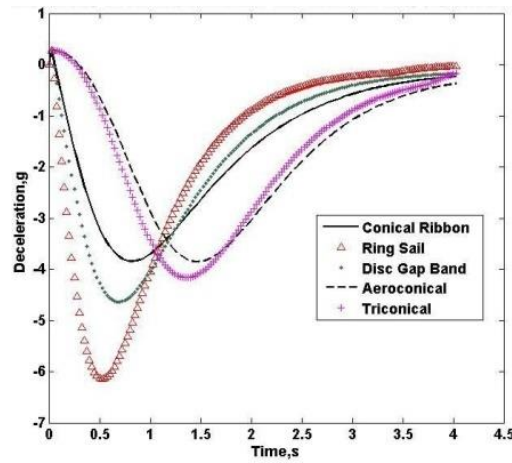


Figure 4.11: Deceleration of different parachutes for 500 kg payload

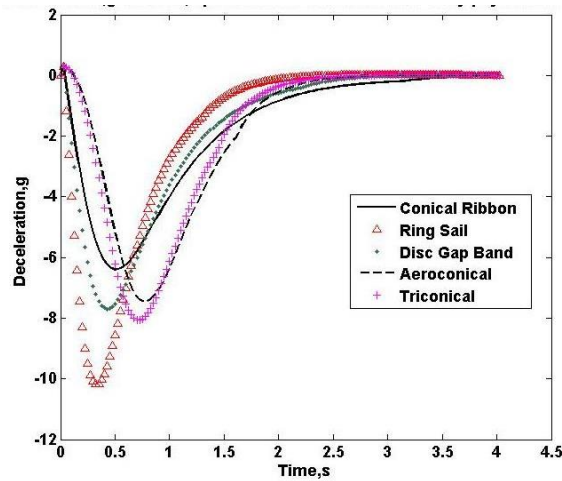


Figure 4.12: Deceleration of different parachutes for 3500 kg payload

In human space recovery programs, the most important factors considered for safe landing are minimum jerk due to parachute opening load, angle of oscillation and quick opening of parachute. The angle of oscillation and canopy filling time of the parachute is also minimum. These properties vary with type of parachutes, whereas peak opening load and

deceleration (g -level) of any type of parachutes can be controlled by introducing reefing. Keeping in view of this, a solid canopy with circumferential and radial slots of equivalent geometric porosity is chosen as shown in Figure 4.13 irrespective of worldwide used ringsail canopy.

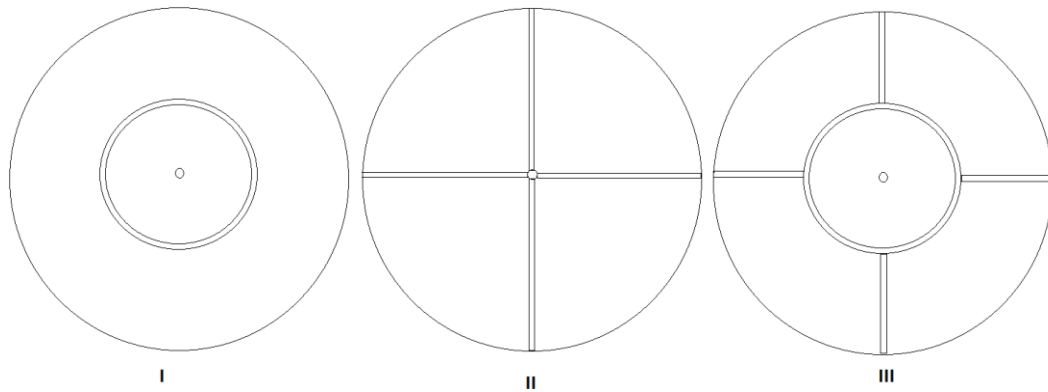


Figure 4.13: Top view of the proposed canopies

Three different shapes of flat circular parachute are proposed in Figure 4.13 which implies that the canopy can have circumferential, radial slots or a combination of both. The geometric porosity of these slits has been kept in limit to avoid any major reduction in drag coefficient of the canopy. Among three proposed canopy shapes, the shape with combination of radial and circumferential slots is chosen ($Cd = 0.75$). This shape is easy in manufacturing in comparison of Ringsail or slotted parachutes. The circumferential slots are made in such a way that the reverse flow field from the slots can be generated similar to the Ringsail parachute. This will nullify the reduction in drag due to slots. A typical gore pattern is shown in Figure 4.14 in which the base of upper gore is made wider than the top of the lower gore.

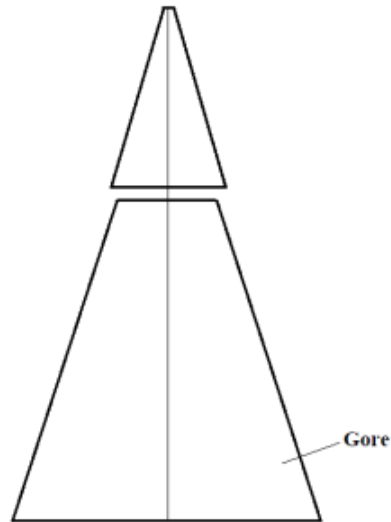


Figure 4.14: Gore layout view

The expected flow field generated with this arrangement is shown in Figure 4.16.

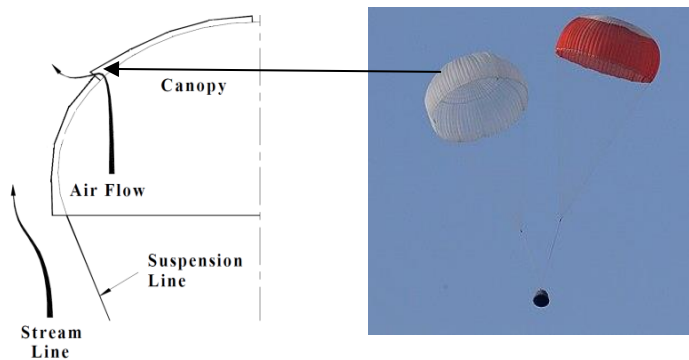


Figure 4.15: Flow field in steady descent

A flat circular canopy with circumferential and radial slots is investigated and will be used for space recovery experiment.

4.4 Summary

An investigation has been carried out on selection and shape of the main parachute canopy for recovery of re-entry space payload of 500 kg (unmanned) and 3500 kg (manned)

classes. Based on the size of the parachute, canopy filling time, velocity reduction, peak deceleration, opening shock, a unique type of solid canopy with slots has been worked out instead of ringsail canopy as used in other missions. Three different slotted configurations on flat circular canopy we proposed. The test results found circular slotted round canopy to yield the best performance compared to the other two options.